HHS Public Access

Author manuscript

*J Nat Prod*. Author manuscript; available in PMC 2016 October 23.

Published in final edited form as:

*J Nat Prod*. 2015 October 23; 78(10): 2471–2480. doi:10.1021/acs.jnatprod.5b00601.

# Angucyclines and Angucyclinones from *Streptomyces* sp. CB01913 Featuring C-ring Cleavage and Expansion

**Ming Ma**[†], **Mostafa E. Rateb**[†], **Qihui Teng**[†], **Dong Yang**[†], **Jeffrey D. Rudolf**[†], **Xiangcheng Zhu**[‡,§], **Yong Huang**[‡], **Li-Xing Zhao**[⊥], **Yi Jiang**[⊥], **Xiuling Li**[‖], **Christoph Rader**[‖,▽], **Yanwen Duan**[‡,§], and **Ben Shen**[*,†,▽,¤]

[†]Department of Chemistry, The Scripps Research Institute, Jupiter, FL 33458, USA

[‡]Xiangya International Academy of Translational Medicine, Central South University, Changsha, Hunan 410013, China

[§]Hunan Engineering Research Center of Combinatorial Biosynthesis and Natural Product Drug Discovery, Changsha, Hunan 410329, China

[⊥]Yunnan Institute of Microbiology, Yunnan University, Kunming, Yunnan 650091, China

[‖]Department of Cancer Biology, The Scripps Research Institute, Jupiter, FL 33458, USA

[▽]Department of Molecular Therapeutics, The Scripps Research Institute, Jupiter, FL 33458, USA

[¤]Natural Products Library Initiative, The Scripps Research Institute, Jupiter, FL 33458, USA

## Abstract

Angucyclines and angucyclinones are aromatic polyketides with a tetracyclic benz[*a*]anthracene skeleton. The benz[*a*]anthracene scaffold is biosynthesized by type II polyketide synthases that catalyze the decarboxylative condensation of a short acyl-CoA starter and nine extender units. Angucyclines and angucyclinones, the largest group of polycyclic aromatic polyketides, achieve structural diversity via subsequent oxidation, ring cleavage, amino acid incorporation, and glycosylation. We here report the discovery of 14 angucyclinones and two angucyclines (**1–16**) from *Streptomyces* sp. CB01913, identifying 12 new compounds featuring various oxidations on rings A and C (**1, 2**, and **4**), different sugar moieties attached to rings A and B (**3** and **6**), and C-ring cleavage (**5** and **10–14**) and expansion (**8**). These new structural features, highlighted by C-ring cleavage and expansion, enrich the structural diversity of angucyclines and angucyclinones. All compounds were tested for cytotoxicity and antibacterial activities, with **1, 5, 15**, and **16** showing moderate activities against selected cancer cell lines or bacterial strains.

[*]To whom correspondence should be addressed: Ben Shen, The Scripps Research Institute, 130 Scripps Way, #3A1, Jupiter, FL 33458; Tel: (561) 228-2456, Fax: (561) 228-2472; shenb@scripps.edu.

**ASSOCIATED CONTENT**

**Supporting Information**. Table S1 summarizes the media A, B, C, and F used for the fermentation of *S.* sp. CB01913. Table S2 provides the primers and PCR conditions of the four housekeeping genes for the phylogenetic analysis. Table S3 compares $^{1}$H NMR data of **7** and **8** with LS1924A[23] in acetone-*d*$_6$. Figure S1 shows the HPLC analysis for the fermentation of *S.* sp. CB01913. Figure S2 shows the phylogenetic analysis for *S.* sp. CB01913. Figures S3–S86 show the NMR, HRESIMS, and IR spectra of compounds **1–14**. The Supporting Information is available free of charge on the ACS Publication website at DOI:.

**Notes**. The authors declare no competing financial interest.

## Graphical abstract

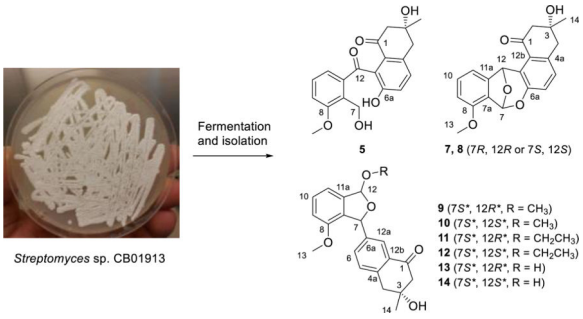


Angucyclines and angucyclinones are aromatic polyketide natural products featuring a tetracyclic benz[*a*]anthracene skeleton that are distinct from the benz[*b*]anthracene skeleton found in tetracyclines and anthracyclines.[1] Since the isolation of tetrangomycin, the first angucyclinone discovered, from *Streptomyces rimosus* in 1965,[2] the angucycline and angucyclinone family of natural products has grown steadily. To date this family of natural products has been discovered exclusively from actinomycetes with *Streptomyces* as the major producers.[1, 2] Representing the largest family of polycyclic aromatic polyketides known to date, angucyclines and angucyclinones feature a characteristic tetracyclic benz[*a*]anthracene scaffold that is biosynthesized by type II polyketide synthases (PKSs) via decarboxylative condensations of a short acyl-CoA starter and nine extender units.[1] The structural diversity of angucyclines and angucyclinones mainly comes from: (i) oxidations on the angular tetracyclic backbone, including hydroxy substitutions at C-4/5/6a/7/12/12a in the saccharothrixins,[3] epoxidation at C-5/6 or C-6a/12a in the panglimycins,[4] or carbonyl substitutions at C-7 and C-12 in the hatomarubigins;[5] (ii) amino acid incorporations, as in the two point attachment of different amino acids to form yet another ring in jadomycins[6] or of tyrosine and tryptophan into urdamycins C and D;[7] (iii) ring cleavages including A-ring cleavage in the grincamycins,[8] B-ring cleavage in the gilvocarcins,[9] or C-ring cleavage in emycins E and F;[10] and (iv) glycosylation at various positions, such as the multiple trisaccharide units of D-olivose-4-1-D-olivose-3-1-L-rhodinose attached at the O-8 position in the landomycins[11] or deoxysugars attached at the O-3 and C-9 positions in the saquayamycins.[12]

As a part of the Natural Products Library Initiative (NPLI) at The Scripps Research Institute (TSRI) dedicated to the discovery of natural products from our Actinomycetales strain collection,[13–17] we report the discovery of 14 angucyclinones and two angucyclines (**1–16**) from *Streptomyces* sp. CB01913, including 12 new compounds with (i) various oxidations on rings A and C (**1, 2**, and **4**), (ii) different glycosylations on rings A and B (**3** and **6**), and (iii) C-ring cleavage (**5** and **10–14**) and expansion (**8**). The natural products isolated in this study show unique characteristics compared with known angucyclines and angucyclinones – (i) **9–14** are the only members with C-ring cleavage between C-12 and C-12a; (ii) **5, 7**, and **8** represent rare C-ring cleavage or expansion between C-6a and C-7; (iii) **3**, with previously reported TAN-1085,[2] represent the only two angucyclines with sugar moieties attached at C-6; and (iv) **1, 4**, and **6** contain a hydroxy group, instead of the usual carbonyl, at C-12. These new structural features, especially the C-ring cleavage and expansion represented by

**5, 8**, and **10–14**, enrich the structural diversity of angucycline and angucyclinone family of natural products. All compounds were tested for cytotoxicity and antibacterial activities, with **1, 5, 15**, and **16** showing moderate activities against selected cancer cell lines or bacterial strains.

## RESULTS AND DISCUSSION

### Strain Selection, Taxonomy, and Fermentation Optimization

The NPLI at TSRI aims at constructing a natural products library with unique chemical and structural diversities that complements TSRI's small molecule collection. The NPLI biases natural products from Actinomycetales that are isolated from unexplored or underexplored ecological niches and unavailable in public strain collections. The current library at TSRI consists of: (i) purified natural products with fully assigned structures, (ii) medium pressure liquid chromatography (MPLC) (on C-18 semipreparative column) fractions, and (iii) extracts. The extracts are generated by fermenting each strain in two media (medium A and medium F, Table S1), and the resultant extracts are subjected to HPLC-photodiode array (PDA)-based chemical profiling, which then guides strain selection for subsequent MPLC fractionation and natural product isolation. Figure S1A depicts HPLC analysis of extracts made from 20 strains in a typical run of fermentation in medium F. Among the 20 strains, *S.* sp. CB01913 was found to produce the most detectable natural products based on chemical profiling as exemplified by the HPLC chromatograms with UV detection at 254 nm. We recently reported methods to guide strain prioritization for natural product discovery by surveying the biosynthetic gene clusters for the targeted class of natural products.[17] While these genomics-based methods are effective in prioritizing strains according to the biosynthetic potential, it is far from certain that the predicted biosynthetic machinery will be functional under the fermentation conditions of investigation for natural product production and isolation. The method reported here, chemical profiling of extracts, complements the genomics-based strain prioritization strategies and allows direct assessment of natural products produced under the conditions of investigation. On the basis of the observed natural product abundance, *S.* sp. CB01913 was selected as a priority strain for natural product isolation.

*S.* sp. CB01913 was isolated from a soil sample collected in Weishan county, Yunnan province, China. It grows well on ISP4 or TSB agar medium. CB01913 was classified as a *Streptomyces* species on the basis of a phylogenetic analysis using the concatenated partial sequences of the four housekeeping genes 16S rRNA, *recA, rpoB*, and *trpB*.[17] As shown in Figure S2, CB01913 clearly lies in the same clade with other *Streptomyces* species.

It is well known that the metabolite profile of a given strain is medium dependent.[17] Thus, we re-fermented *S.* sp. CB01913 in four media (medium A, B, C, and F, Table S1). HPLC-PDA analysis showed that *S.* sp. CB01913 yielded the richest metabolite profile in medium B among the four media examined, as exemplified by the HPLC chromatograms with UV detection at 254 nm (Figure S1B). Medium B was selected for large-scale fermentation of *S.* sp. CB01913, from which the 16 compounds, including 12 new ones (**1–6, 8**, and **10–14**), were isolated.

## Structural Elucidation

Compound **1** was obtained as a brown powder. High-resolution electro-spray ionization mass spectrometry (HRESIMS) analysis afforded an $[M + H]^+$ ion at *m/z* 339.1226, giving the molecular formula of **1** as $C_{20}H_{18}O_5$. The $^1H$, $^{13}C$, and COSY NMR spectra of **1** resembled those of 8-*O*-methyltetrangomycin (**16**)[18a, 18b] (Figure 1), except that the resonances at $\delta_H$ 6.39 (s, H-12) (Table 1) and $\delta_C$ 64.3 (C-12) (Table 4), attributed to a methine group in **1**, replaced the resonance at $\delta_C$ 184.5 (C-12), attributed to a carbonyl group in **16**. These differences indicated one of the carbonyl groups at C-7 or C-12 in **16** was reduced to a hydroxy group in **1**. The correlations of H-12 with C-11 and C-12b, H-11 with C-12, and H-6 with C-7 in the HMBC spectrum of **1** identified the hydroxy substitution at C-12 (Figure 1). On that basis, compound **1** was identified as 12-deoxo-12-hydroxy-8-*O*-methyltetrangomycin through the relative configuration between C-3 and C-12 was not established (Figure 1).

Compound **2** was obtained as a yellow powder. HRESIMS analysis afforded an $[M + H]^+$ ion at *m/z* 353.1020, giving the molecular formula of **2** as $C_{20}H_{16}O_6$. The chemical shifts and coupling systems in the $^1H$, $^{13}C$, and COSY NMR spectra of **2** resembled those of **16**, except that the resonances attributed to the methylene group at C-4 in **16** were replaced by resonances at $\delta_H$ 4.72 (s, H-4) (Table 1) and $\delta_C$ 73.8 (C-4) (Table 4) attributed to one methine group in **2**, indicating that the only difference between **2** and **16** was one additional hydroxy group at C-4 in **2**. The correlations of H-2 with C-1 and C-4, H-14 with C-4, and H-4 with C-4a in the HMBC spectrum of **2** confirmed the hydroxy substitution at C-4 (Figure 1). Among all natural angucyclines and angucyclinones known to date, the configuration of the methyl and hydroxy groups at C-3, as drawn in Figure 2, is absolutely conserved. Because the absolute *R*-configuration at C-3 of the co-purified **16** has been confirmed by total synthesis,[18c] the absolute configuration of C-3 in **2** was assigned as *S* based on their shared biosynthetic origin. This assignment was further supported by the NOESY spectrum of **2** – the correlations of H-4 with $H_a$-2, $H_3$-14 with both H-4 and $H_a$-2, and 3-OH group with $H_b$-2 unambiguously established that $H_3$-14, H-4, and $H_a$-2 were on the same face of ring A, with $H_b$-2 and the 3- and 4-OH groups lying on the opposite face of ring A (Figure 2). Taken together, the absolute configuration of C-4 in **2** was assigned as *R*, and **2** was identified as 4*R*-hydroxy-8-*O*-methyltetrangomycin.

Compound **3** was obtained as a green-yellow powder. HRESIMS analysis afforded an $[M + H]^+$ ion at *m/z* 499.1590, giving the molecular formula of **3** as $C_{26}H_{26}O_{10}$. Comparison of the $^1H$ and COSY NMR spectra between **3** and **16**[18a, 18b] showed that the AB coupling system of H-5 with H-6 in ring B of **16** was replaced by a methine singlet at $\delta_H$ 7.38 (s, H-5) and resonances attributed to a 6-deoxysugar moiety at $\delta_H$ 5.66 (br s, H-1'), $\delta_H$ 3.98 (dd, $J$ = 3.2, 1.8 Hz, H-2'), $\delta_H$ 3.90 (dd, $J$ = 9.5, 3.2 Hz, H-3'), $\delta_H$ 3.36 (t, $J$ = 9.4 Hz, H-4'), $\delta_H$ 3.55 (m, H-5') and $\delta_H$ 1.13 (d, $J$ = 6.2 Hz, $H_3$-6') were observed in **3** (Table 2). Comparison of chemical shifts, coupling patterns, and correlations of resonances attributed to this sugar moiety in the $^1H$, $^{13}C$, COSY, and HSQC NMR spectra (Figure 1 and Tables 2 and 4) with literature data,[19] in combination with the correlations in the NOESY spectrum (Figure 2), identified the sugar as an α-rhamnose. The absolute configuration of the L-rhamnose moiety was assigned on the basis of a common biosynthetic pathway shared with **6** (see structural

elucidation of **6**). In the HMBC spectrum of **3**, the correlations of H-1' with C-6, H-5 with C-6a, C-12b, and C-4, and H-4 with C-5 identified the attachment of α-L-rhamnose at C-6 (Figure 1). Therefore, compound **3** was identified as 6-*O*-α-L-rhamnosyl-8-*O*-methyltetrangomycin.

Compound **4** was obtained as a colorless gum. HRESIMS analysis afforded an $[M + Na]^+$ ion at *m/z* 381.1306, giving the molecular formula of **4** as $C_{20}H_{22}O_6$. The $^1H$ and COSY NMR spectra of **4** showed similar resonances, attributed to one methyl group and two methylene groups at ring A, one methoxy group, and an ABC coupling system at ring D, with those in **16**. However, the resonances for an AB coupling system of aromatic methine groups at ring B in **16** shifted to $\delta_H$ 6.03 (d, $J$ = 10.1 Hz, H-5) and $\delta_H$ 6.31 (d, $J$ = 10.1 Hz, H-6) in **4**. In addition, **4** showed two more methine group resonances at $\delta_H$ 4.83 (br d, $J$ = 9.7 Hz, H-7) and $\delta_H$ 4.86 (br s, H-12) that were coupled with the two hydroxy resonances at $\delta_H$ 5.24 (br d, $J$ = 9.3 Hz, 7-OH) and $\delta_H$ 5.48 (br s, 12-OH), one more aliphatic methine group at $\delta_H$ 2.67 (br s, H-12a), and one more hydroxy resonance at $\delta_H$ 5.15 (br d, $J$ = 9.3 Hz, 6a-OH) (Table 1). The $^{13}C$ NMR spectrum of **4**, compared to that of **16**, showed that the two carbonyl resonances at C-7 and C-12 and the two aromatic carbon resonances at C-6a and C-12a in **16** were replaced by three aliphatic methine and one aliphatic non-protonated carbon resonances in **4** (Table 4). These differences suggested that the two carbonyl groups in **16** were reduced to two hydroxy groups and the double bond at C-6a/12a in **16** was reduced to a saturated bond, respectively, in **4**. These were confirmed by the correlation of 12-OH with H-12a in the COSY spectrum, and the correlations of 6a-OH with C-7, H-7 with C-8, H-12a with C-1 and C-6, H-12 with C-12a, and H-11 with C-12 in the HMBC spectrum of **4**, which also established the attachment of the hydroxy groups at C-6a, C-7 and C-12 (Figure 1). Finally, the relative configuration of **4** was solved by a NOESY experiment – correlations of H-6 with H-7 and 7-OH suggested that the C-6a/C-6 bond took an equatorial conformation, the correlations of the axial 6a-OH with both H-7 and H-12a suggested that 6a-OH, H-7 and H-12a were on the same side of ring C, and the correlations of H-12a with H-12, 12-OH with H-6 suggested that H-12 and H-12a were on the same side of ring C (Figure 2). Taken all together, compound **4** was identified as another congener of **16**, and the relative configuration at C-6a, C-7, C-12 and C-12a in **4** was assigned as *S*, S*, S** and *S**, respectively.

Compound **5** was obtained as a green-yellow powder. HRESIMS analysis afforded an $[M + Na]^+$ ion at *m/z* 379.1161, giving the molecular formula of **5** as $C_{20}H_{20}O_6$. The $^1H$ and $^{13}C$ NMR spectra of **5** resembled those of angucyclinone C,[20] except for one hydroxy resonance occurring at $\delta_H$ 9.89 (s, 6a-OH) in the $^1H$ NMR spectrum of **5** (Table 1). This difference in combination with the molecular formula of **5** indicated that the ether ring in angucyclinone C was oxidatively cleaved in **5**. This was confirmed by the correlations of 6a-OH with C-6, C-6a and C-12a and of H-7 with C-8 and C-11a in the HMBC spectrum (Figure 1). Thus compound **5** was identified as the C-ring cleavage product of angucyclinone C.

Compound **6** was obtained as a yellow powder. HRESIMS analysis afforded an $[M + H]^+$ ion at *m/z* 467.1691, giving the molecular formula of **6** as $C_{26}H_{26}O_8$. The chemical shifts and coupling systems in the $^1H$ and COSY NMR spectra of **6** resembled those of

pseudonocardone A[21] except the resonances attributed to one 6-deoxysugar moiety instead of the β-glucuronic acid moiety in pseudonocardone A (Table 2). The sugar moiety was identified as α-rhamnose by methods similar to those described for **3** (Tables 2 and 4), and the absolute configuration of L-rhamnose was established upon mild acid hydrolysis followed by optical rotation comparison with literature value.[22] The different chemical shifts of H-2' and C-3' between **3** and **6** are due to the different sugar moiety environments. This is supported by the strong correlations between H-12 with H-2' and H-3' in the NOESY spectrum of **6** (Figure 2). The correlations of H-1' with C-1, 12-OH with C-11a and C-12a, H-12 with C-12b, and H-6 with C-7 in the HMBC spectrum of **6** identified the attachment of α-L-rhamnose at C-1 and the hydroxy group at C-12 (Figure 1). The absolute configuration at C-12 was not assigned. Compound **6** was thus identified as 1-*O*-α-L-rhamnosyl-12-hydroxy-8-*O*-methyltetrangulol.

Compounds **7** and **8** were obtained as yellow powders. HRESIMS analysis for **7** and **8** afforded the same $[M + H]^+$ ion at *m/z* 339.1225, giving the molecular formula of **7** and **8** as $C_{20}H_{18}O_5$. Analysis for the $^1H$, $^{13}C$, COSY, HSQC, and HMBC NMR spectra of **7** and **8** (Figure 1) showed that they had the same planar structure as LS1924, a known angucyclinone isolated from *Streptomyces* sp. LS1924 with its absolute configuration unassigned.[23] However, **7** and **8** had distinct chemical shifts for H-11 and H-12 in their $^1H$ NMR spectra, indicating that **7** and **8** are isomers with different configurations at C-7 and C-12 (*R, R* or *S, S*) (Table 1). Comparison of the $^1H$ NMR spectra of **7, 8**, and LS1924A in acetone-$d_6$ clearly showed that **7** had nearly identical resonances at $\delta_H$ 6.76 (s, H-7), 6.72 (s, H-12), and 7.21 (d, $J$ = 7.2 Hz, H-11) to those of LS1924A, while **8** had distinct resonances at $\delta_H$ 6.84 (s, H-7), 6.76 (s, H-12), and 7.14 (d, $J$ = 7.2 Hz, H-11) (Table S3). These data supported the final assignment of **7** as LS1924A and **8** as a diastereomer of LS1924A (i.e., **7**), respectively.

Compounds **9–14** were obtained as white powders. HRESIMS analysis for **9** and **10** afforded the same $[M + Na]^+$ ion at *m/z* 377.1358, giving the molecular formula of **9** and **10** as $C_{21}H_{22}O_5$. Analysis of the $^1H$, $^{13}C$, COSY, HSQC, and HMBC NMR spectra of **9** showed that it was same as the angucyclinone from *Streptomyces* sp. M268 (Tables 3 and 5).[24] However, close examination of the NMR spectra of **9** indicated that the relative configuration of the angucyclinone from *S.* sp. M268 was incorrectly assigned. In the NOESY spectrum of **9**, the correlations of H-7 with both H-15 and H-12a, H-12 with H-12a, which was similar to that of the angucyclinone from *S.* sp. M268,[24] suggested that H-7 and H-12 adopted "*trans*" positions on the different sides of the five-membered ether ring (Figure 2). Thus, we assigned the relative configuration of **9**, thereby correcting the assignment for the angucyclinone from *S.* sp. M268, at C-7 and C-12 as *S** and *R**, respectively.

Compound **10** had nearly identical $^1H$, $^{13}C$, COSY, HSQC, and HMBC NMR spectra with **9** except that the proton resonance attributed to H-12 shifted from $\delta_H$ 6.43 in **9** to $\delta_H$ 6.13 in **10** (Figure 1 and Tables 3 and 5), indicating that **10** has only a different configuration at C-12 compared with **9**. In the NOESY spectrum of **10**, the correlation of $H_3$-15, instead of H-12, with H-12a established H-7 and H-12 adopted the "*cis*" positions on the same side of the

five-membered ether ring (Figure 2). Therefore the relative configuration at C-7 and C-12 in **10** was established as *S** and *S**, respectively. Compounds **11** and **12** were identified as derivatives of **9** and **10**, respectively, with the methoxy group at C-12 replaced by one ethoxy group based on their $^{1}H$, $^{13}C$, COSY, HSQC, HMBC, and NOESY NMR spectra (Figures 1 and 2 and Tables 3 and 5). Compounds **13** and **14** were also identified as derivatives of **9** and **10**, respectively, with the methoxy group at C-12 replaced by one hydroxy group based on their $^{1}H$, $^{13}C$, COSY, HSQC, HMBC, and NOESY NMR spectra (Figures 1 and 2 and Tables 3 and 5). However, **13** and **14** undergo a rapid equilibrium, via $H_2O$ attacking at the hemiacetal group, to afford a mixture with equal amount of **13** and **14**, giving rise to two sets of resonances in their NMR spectra. As **13** and **14** rapidly equilibrate in the presence of $H_2O$, we cannot rule out the possibility of both **9**/**10** and **11**/**12** pairs as isolation artifacts of **13**/**14** in the presence methanol and ethanol, respectively.

Compounds **15** and **16** were identified as tetrangomycin[25] and 8-*O*-methyltetrangomycin,[18a, 18b] respectively, based on the comparison of their NMR and MS data with previously published data.

## Bioactivity Assays

Angucyclines and angucyclinones are known for their cytotoxicity and antibacterial activities. They are both reported to possess $IC_{50}$ values between 1 μM and 100 μM against various cancer cell lines.[1, 2, 8, 21] In this study, five cancer cell lines, human glioblastoma multiforme SF295, human glioblastoma SF539, human lung squamous carcinoma H226, human melanoma M14, and human breast adenocarcinoma MDA-MB-468, were chosen to test the cytotoxicities of **1–16**, using mitomycin C as the positive control. Compounds **1** was active against the SF295 and H226 cell lines, and compound **15** and **16** were active against the H226, SF539, and M14 cell lines (Table 6), while the rest were inactive ($IC_{50}$ > 10 μM). The potencies for **15** and **16** against the five cell lines tested in this study were similar to other cancer cell lines reported previously.[22, 26, 27]

The angucycline and angucyclinone family of natural products selectively inhibit Gram-positive bacteria.[2,28–31] Compounds **1–16** were tested against the Gram-positive *Staphylococcus aureus* ATCC 25923, *Bacillus subtilis* ATCC 23857, and *Mycobacterium smegmatis* ATCC 607 and the Gram-negative *Escherichia coli* ATCC 25922 and *E. coli* JM109, using tetracycline as the positive control. As summarized in Table 5, both **15** and **16** showed moderate activity against *S. aureus* ATCC 25923, *B. subtilis* ATCC 23857, and *M. smegmatis* ATCC 607, with the minimum inhibitory concentration (MIC) values ranging from 8.1 to 25 μg/mL, which were similar to the reported MIC values for **15** and **16** against other *S. aureus* or *B. subtilis* species.[26, 27, 32–34] Compound **5** showed weak activity against *B. subtilis* ATCC 23857 and *M. smegmatis* ATCC 607. As previously observed for known angucyclines and angucyclinones,[2] **1–16** showed no activity against the Gram-negative *E. coli* ATCC 25922 and JM109 species.

In conclusion, we isolated 14 angucyclinones and two angucyclines (**1–16**), including 12 new compounds (**1–6, 8**, and **10–14**), from *S.* sp. CB01913, a strain selected based on chemical profiling and fermentation optimization. The new compounds featured unusual

structural properties including various oxidations on rings A and C (**1, 2** and **4**), different sugar moieties attached to rings A and B (**3** and **6**), and C-ring cleavage (**5** and **10–14**) and expansion (**8**). Cytotoxicity and antibacterial assays showed that **1, 5, 15**, and **16** gave moderate inhibitory activities against selected cancer cell lines and bacterial strains, respectively. The new structural features, especially C-ring cleavage and expansion disrupting the conjugated system spanning rings B, C, and D, enrich the structural diversity of angucyclines and angucyclinones, and set the stage to further evaluate the structure-activity-relationships of this family of aromatic polyketide natural products.

## EXPERIMENTAL SECTION

### General Experimental Procedures

Optical rotations were measured with an AUTOPOL IV automatic polarimeter (Rudolph Research Analytical). UV spectra were collected with a NanoDrop 2000C spectrophotometer (Thermo Scientific). IR spectra were collected with a Spectrum One FT-IR spectrometer (PerkinElmer). NMR data was collected on a Bruker 700 MHz/54mm Ultra Shield Magnet System. HRESIMS data was collected on a Thermo Finnigan LTQ Orbitrap mass spectrometer. MPLC separation was conducted on a Biotage Isolera One using a KP-C18-HS (30 g) column. Size exclusion chromatography was performed on Sephadex LH-20 (GE Healthcare) columns. HPLC was carried out on a Varian semipreparative HPLC system (Woburn, MA) equipped with a Prostar 330 detector, using a GRACE Apollo $C_{18}$ column ( 250 mm × 4.6 mm, 5 μm) for analysis and an Alltima $C_{18}$ column (250 mm × 10.0 mm, 5 μm) for purification. All fermentations were carried out in New Brunswick Scientific Innova 44 incubator shakers or New Brunswick BioFlo/celliGen 115 fermentors. Diaion HP-20 resin was purchased from Sigma-Aldrich.

### Strain Isolation and Identification

Strain *Streptomyces* sp. CB01913 was isolated from a soil sample collected in Weishan county (location: 25°23' N, 100°33' E). The strain was purified with standard diluting plate method,[35] using agar plates with medium consists of glycerol 10 g, asparagine 1 g, $K_2HPO_4{\cdot}H_2O$ 1 g, $MgSO_4{\cdot}7H_2O$ 0.5 g, $CaCO_3$ 0.3 g, vitamin mixture (thiamine-HCl 0.5 mg, riboflavin 0.5 mg, niacin 0.5 mg, pyridoxine 0.5 mg, calcium pantothenate 0.5 mg, inositol 0.5 mg, 4-aminobenzoic acid 0.5 mg, and biotin 0.25 mg), and agar 15 g, in 1 L $H_2O$, pH 7.7. The strain was preserved as spore suspension (20% glycerol, v/v) at −80 °C.

The strain CB01913 was grown on ISP4 medium at 28 °C for 7 days. The spores were harvested and cultured in TSB at 28 °C for 2 days, after which the genomic DNA was isolated following standard protocols.[17] Four housekeeping genes, 16S rRNA, *recA* (encoding recombinase A), *rpoB* (encoding RNA polymerase β subunit), and *trpB* (encoding tryptophan synthase β subunit), were amplified by PCR, sequenced, and deposited into GenBank under accession numbers KT581419, KT581420, KT581421, and KT581422, respectively. One Taq Quick-Load 2× Master Mix (New England BioLabs Inc) was used for PCR amplification (PCR primers and PCR conditions were listed in Table S2), and QIAquick Gel Extraction Kit and QIAprep Spin Miniprep Kit (Qiagen) were used for PCR product recovery. The PCR products were sequenced and the resulting sequences were used

for BLAST on the NCBI website to search for the homologous gene candidates, which were then used as the representative *Streptomyces* spp. in the phylogenetic tree, assigning CB01913 as a *Streptomyces* species (Figure S2).[17]

## Fermentation and Isolation

*S.* sp. CB01913 was grown on ISP4 medium (Difco) for sporulation. After one week, the spores were harvested and 1 mL of spore suspension was added into 600 mL of seed medium (Tryptic Soy Broth) (Bacto); incubation continued on a rotary shaker with 250 rpm at 28 °C for 2 days. The resultant seed culture (600 mL) was then inoculated into 8 L production medium [dextrin (Sigma-Aldrich) 40 g, tomato paste (Plant Media) 7.5 g, N-Z-Amine A (Sigma-Aldrich) 2.5 g, primary yeast (Acros Organics) 5 g, in 1.0 L deionized $H_2O$, pH 7.0), in a 14 L fermentor, and the fermentation continued with 250 rpm at 28 °C for 7 days. After fermentation, 400 g of Diaion HP-20 resin were added into the medium and stirred overnight. The resin and the cell mass were harvested by centrifugation, washed by deionized $H_2O$, and extracted with MeOH. The MeOH extract was concentrated in vacuo, and the residue was loaded onto a Biotage SNAP Cartridge KP-C18-HS column (30 g) and separated by MPLC using an increasing gradient of 5% MeOH in $H_2O$ to 80% MeOH in $H_2O$ as the mobile phase. The flowrate was 20 mL/min and every 35 mL was collected as a fraction. In total, 35 fractions (m1 to m35) were collected. All 35 fractions were analyzed by HPLC. Fraction m20 was further purified by preparative HPLC using $CH_3CN/H_2O$ (32/68) as the mobile phase, with UV detection at 254 nm, to afford **1** (11.7 mg) and **16** (15.1 mg). Fraction m17 was further purified by preparative HPLC using $CH_3CN/H_2O$ (27/73) as the mobile phase with UV detection at 210 nm to afford **2** (3.4 mg). Fraction m8 was further purified by Sephadex LH-20 column using MeOH as the mobile phase to give four subfractions s1-s4, of which s2 was further purified by preparative HPLC using $CH_3CN/H_2O$ (27/73) as the mobile phase with UV detection at 300 nm to afford **4** (0.9 mg). Fraction m14 was further purified by preparative HPLC using $CH_3CN/H_2O$ (27/73) as the mobile phase with UV detection at 260 nm to afford **3** (5.1 mg) and **5** (8.7 mg). Fraction m27 was further purified by preparative HPLC using $CH_3CN/H_2O$ (45/55) as the mobile phase with UV detection at 254 nm to afford **6** (7.2 mg), **7** (1.5 mg), **8** (1.6 mg), and **15** (4.5 mg). Fraction m9 was further purified by preparative HPLC using an increasing gradient of 30% $CH_3CN$ in $H_2O$ to 50% $CH_3CN$ in $H_2O$ over 20 min, then 50% $CH_3CN$ in $H_2O$ over 5 min as the mobile phase, with UV detection at 254 nm to afford **9** (7.7 mg), **10** (0.6 mg), **11** (2.6 mg), **12** (3.0 mg), **13** (3.7 mg), and **14** (3.5 mg). All preparative HPLC was carried out at a flowrate of 3 mL/min.

**Compound 1—***Compound 1*: brown powder; $[\alpha]_D^{27}$ – 133 (*c* 0.34, DMSO); UV (DMSO) $\lambda_{max}$ (log ε) 254 (4.13), 334 (3.66) nm; IR $\nu_{max}$ 3441, 2933, 1667, 1595, 1470, 1271, 1236, 1124, 1072, 1022, 966, 819, 757, 723 $cm^{-1}$; $^1H$ NMR (700 MHz) data, Table 1; $^{13}C$ NMR (175 MHz) data, Table 4; HRESIMS *m/z* 339.1226 $[M + H]^+$ (calcd for $C_{20}H_{18}O_5$, 339.1231).

**Compound 2—***Compound 2*: yellow powder; $[\alpha]_D^{27}$ – 76.7 (*c* 0.18, DMSO); UV (DMSO) $\lambda_{max}$ (log ε) 266 (4.26), 373 (3.52) nm; IR $\nu_{max}$ 3663, 3390, 2972, 2901, 1744, 1700, 1670, 1589, 1472, 1443, 1406, 1394, 1382, 1265, 1230, 1065, 1056, 956, 892, 822,

719 $cm^{-1}$; $^{1}H$ NMR (700 MHz) data, Table 1; $^{13}C$ NMR (175 MHz) data, Table 4; HRESIMS *m/z* 353.1020 $[M + H]^+$ (calcd for $C_{20}H_{16}O_6$, 353.1024).

**Compound 3—***Compound* ***3***: green-yellow powder; $[\alpha]_D^{27}$ – 43.0 (*c* 0.25, DMSO); UV (DMSO) $\lambda_{max}$ (log ε) 261 (4.20), 371 (3.52) nm; IR $\nu_{max}$ 3663, 3391, 2971, 2901, 1671, 1591, 1406, 1394, 1382, 1251, 1231, 1065, 1056, 892, 880 $cm^{-1}$; $^{1}H$ NMR (700 MHz) data, Table 2; $^{13}C$ NMR (175 MHz) data, Table 4; HRESIMS *m/z* 499.1590 $[M + H]^+$ (calcd for $C_{26}H_{26}O_{10}$, 499.1602).

**Compound 4—***Compound* ***4***: colorless gum; $[\alpha]_D^{27}$ – 4.2 (*c* 0.07, DMSO); UV (DMSO) $\lambda_{max}$ (log ε) 284 (3.79), 304 (3.72) nm; IR $\nu_{max}$ 3277, 2937, 2838, 1645, 1591, 1480, 1437, 1416, 1310, 1266, 1177, 1112, 1092, 1012, 951, 857, 764 $cm^{-1}$; $^{1}H$ NMR (700 MHz) data, Table 1; $^{13}C$ NMR (175 MHz) data, Table 4; HRESIMS *m/z* 381.1306 $[M + Na]^+$ (calcd for $C_{20}H_{22}O_6$, 381.1313).

**Compound 5—***Compound* ***5***: green-yellow powder; $[\alpha]_D^{27}$ – 1.12 (*c* 0.36, DMSO); UV (DMSO) $\lambda_{max}$ (log ε) 252 (4.20), 328 (3.68) nm; IR $\nu_{max}$ 3663, 3440, 3290, 2980, 2902, 1778, 1676, 1607, 1586, 1489, 1454, 1405, 1394, 1298, 1266, 1056, 1020, 951, 900, 824, 780 $cm^{-1}$; $^{1}H$ NMR (700 MHz) data, Table 1; $^{13}C$ NMR (175 MHz) data, Table 4; HRESIMS *m/z* 379.1161 $[M + Na]^+$ (calcd for $C_{20}H_{20}O_6$, 379.1156).

**Compound 6—***Compound* ***6***: yellow powder; $[\alpha]_D^{27}$ – 122 (*c* 0.23, DMSO); UV (DMSO) $\lambda_{max}$ (log ε) 274 (4.31), 334 (3.83) nm; IR $\nu_{max}$ 3663, 3403, 2973, 2902, 1650, 1596, 1454, 1406, 1394, 1383, 1268, 1231, 1075, 1065, 1051, 955, 892, 807, 764 $cm^{-1}$; $^{1}H$ NMR (700 MHz) data, Table 2; $^{13}C$ NMR (175 MHz) data, Table 4; HRESIMS *m/z* 467.1691 $[M + H]^+$ (calcd for $C_{26}H_{26}O_8$, 467.1704).

**Compound 7—***Compound* ***7***: yellow powder; $[\alpha]_D^{27}$ + 250 (*c* 0.07, DMSO); UV (DMSO) $\lambda_{max}$ (log ε) 261 (3.72), 326 (3.42) nm; IR $\nu_{max}$ 3663, 2993, 2958, 2903, 1735, 1453, 1404, 1393, 1382, 1250, 1230, 1083, 1035, 956, 893, 871 $cm^{-1}$; $^{1}H$ NMR (700 MHz) data, Table 1; $^{13}C$ NMR (175 MHz) data, Table 4; HRESIMS *m/z* 339.1225 $[M + H]^+$ (calcd for $C_{20}H_{18}O_5$, 339.1231).

**Compound 8—***Compound* ***8***: yellow powder; $[\alpha]_D^{27}$ – 310 (*c* 0.08, DMSO); UV (DMSO) $\lambda_{max}$ (log ε) 261 (3.78), 329 (3.46) nm; IR $\nu_{max}$ 3675, 3375, 2972, 2902, 1677, 1614, 1598, 1485, 1469, 1436, 1407, 1380, 1276, 1242, 1076, 1047, 960, 924, 895, 820, 774 $cm^{-1}$; $^{1}H$ NMR (700 MHz) data, Table 1; $^{13}C$ NMR (175 MHz) data, Table 4; HRESIMS *m/z* 339.1225 $[M + H]^+$ (calcd for $C_{20}H_{18}O_5$, 339.1231).

**Compound 9—***Compound* ***9***: white powder; $[\alpha]_D^{27}$ – 63.6 (*c* 0.35, DMSO); UV (DMSO) $\lambda_{max}$ (log ε) 252 (3.95), 297 (3.26) nm; IR $\nu_{max}$ 3663, 2971, 2901, 1678, 1611, 1453, 1405, 1393, 1382, 1251, 1231, 1065, 1056, 957, 892, 880, 871 $cm^{-1}$; $^{1}H$ NMR (700 MHz) data, Table 3; $^{13}C$ NMR (175 MHz) data, Table 5; HRESIMS *m/z* 377.1358 $[M + Na]^+$ (calcd for $C_{21}H_{22}O_5$, 377.1364).

**Compound 10—***Compound **10***: white powder; $[\alpha]_D^{27}$ + 49 (*c* 0.01, DMSO); UV (DMSO) $\lambda_{max}$ (log ε) 252 (3.93), 297 (3.21) nm; IR $\nu_{max}$ 3663, 2981, 2902, 1682, 1608, 1453, 1406, 1394, 1383, 1251, 1231, 1067, 1057, 893 $cm^{-1}$; $^1H$ NMR (700 MHz) data, Table 3; $^{13}C$ NMR (175 MHz) data, Table 5; HRESIMS *m/z* 377.1358 $[M + Na]^+$ (calcd for $C_{21}H_{22}O_5$, 377.1364).

**Compound 11—***Compound **11***: white powder; $[\alpha]_D^{27}$ – 56.5 (*c* 0.18, DMSO); UV (DMSO) $\lambda_{max}$ (log ε) 254 (4.00), 297 (3.33) nm; IR $\nu_{max}$ 3661, 3414, 2974, 2901, 1683, 1611, 1486, 1439, 1406, 1377, 1319, 1270, 1230, 1190, 1076, 1068, 1053, 1004, 961, 923, 822, 777 $cm^{-1}$; $^1H$ NMR (700 MHz) data, Table 3; $^{13}C$ NMR (175 MHz) data, Table 5; HRESIMS *m/z* 391.1513 $[M + Na]^+$ (calcd for $C_{22}H_{24}O_5$, 391.1520).

**Compound 12—***Compound **12***: white powder; $[\alpha]_D^{27}$ + 46.7 (*c* 0.18, DMSO); UV (DMSO) $\lambda_{max}$ (log ε) 254 (4.13), 297 (3.32) nm; IR $\nu_{max}$ 3663, 3398, 2971, 2895, 1683, 1610, 1487, 1439, 1405, 1376, 1349, 1321, 1269, 1231, 1103, 1076, 1052, 1002, 955, 823, 780 $cm^{-1}$; $^1H$ NMR (700 MHz) data, Table 3; $^{13}C$ NMR (175 MHz) data, Table 5; HRESIMS *m/z* 391.1512 $[M + Na]^+$ (calcd for $C_{22}H_{24}O_5$, 391.1520).

**Compounds 13+14 (equal amount)—***Compounds **13+14*** (equal amount): white powder; $[\alpha]_D^{27}$ – 9.1 (*c* 0.34, DMSO); UV (DMSO) $\lambda_{max}$ (log ε) 254 (3.97), 297 (3.29) nm; IR $\nu_{max}$ 3340, 2965, 1681, 1610, 1486, 1433, 1270, 1231, 1191, 1144, 1104, 1051, 1002, 945, 923, 824, 777 $cm^{-1}$; $^1H$ NMR (700 MHz) data, Table 3; $^{13}C$ NMR (175 MHz) data, Table 5; HRESIMS *m/z* 363.1203 $[M + Na]^+$ (calcd for $C_{20}H_{20}O_5$, 363.1207).

**Compound 15—***Compound **15***: yellow powder; $[\alpha]_D^{27}$ – 119 (*c* 0.32, DMSO) {$[\alpha]_D^{20}$ – 85.6 (*c* 0.49, $CHCl_3$)[25b]}; UV (DMSO) $\lambda_{max}$ (log ε) 266 (4.32), 396 (3.58) nm; IR $\nu_{max}$ 3671, 2973, 2902, 1704, 1637, 1591, 1455, 1405, 1394, 1382, 1264, 1159, 1075, 1049, 892, 722 $cm^{-1}$.

**Compound 16—***Compound **16***: yellow powder; $[\alpha]_D^{27}$ – 132 (*c* 0.34, DMSO) {$[\alpha]_D^{20}$ – 140 (*c* 0.04, MeOH)[18b]}; UV (DMSO) $\lambda_{max}$ (log ε) 266 (4.40), 375 (3.64) nm; IR $\nu_{max}$ 3484, 2971, 1702, 1670, 1592, 1471, 1303, 1269, 1119, 1071, 1022, 958, 820, 722 $cm^{-1}$.

## Determination of Sugar Absolute Configuration

To determine the absolute configuration of the α-L-rhamnose, **6** (3.0 mg) was first dissolved in 500 μL of acetone, followed by the addition of 4 mL of 2% $H_2SO_4$. The resulting solution was stirred at 90 °C for 4 h, and complete hydrolysis was confirmed by HPLC and TCL analysis. After cooling down to room temperature, the hydrolysis mixture was first extracted by 6 mL of $CHCl_3$, and the aqueous layer was then neutralized to pH 7.0 with $NaHCO_3$ and concentrated in vacuum to afford a white solid. The white solid was dissolved in 1 mL of $H_2O$ and subjected to the optical rotation dispersion (ORD) determination. The observed ORD value of $[\alpha]_D^{27}$ +7.5 (c 0.10, $H_2O$) agreed with the reported ORD value of $[\alpha]_D^{25}$ +10.2 (c 0.20, $H_2O$),[22] thereby establishing the sugar in **6** as L-rhamnose.

### Biological Assays

The *S. aureus* ATCC 25923, *B. subtilis* ATCC 23857, *E. coli* ATCC 25922, and *M. smegmatis* ATCC 607 strains, as well as the human breast adenocarcinoma MDA-MB-468 were purchased from American Type Culture Collection (ATCC). *E. coli* JM109 was purchased from Promega corporation. The human glioblastoma multiforme SF295, human glioblastoma SF539 and human lung squamous carcinoma H226 were purchased from the Cell Based Screening Core of TSRI Florida. The human melanoma M14 was kindly provided by Dr. Min Guo from the Department of Cancer Biology, TSRI Florida. The cytotoxicity assay was carried out using the standard protocol from the Promega website (https://www.promega.com/resources/protocols/technical-bulletins/0/celltiter-96-aqueous-one-solution-cell-proliferation-assay-system-protocol/), with the CellTiter 96 Aqueous One Solution Proliferation Assay (MTS) Kit (Promega). Cells were plated in 96-well plates at 5,000 cells/well in RPMI 1640 medium (ThermFisher) and allowed to adhere overnight at 37 °C in a humidified atmosphere of 5% $CO_2$. Medium was then removed and replaced by fresh RPMI 1640 medium containing different concentrations of different compounds. The cells were treated for 72 h before the assay was developed. All assay values were measured in triplicate. The $IC_{50}$ values were determined using GraphPad/Prism software.

The antibacterial activities were first assessed by inhibition zones using the agar diffusion method.[36] Each compound (25 μL), prepared to a concentration of 2 mM in $H_2O$, was dropped onto the filter paper on the tryptic soy agar plate. The plate was incubated at 37 °C for 12 h, after which the inhibition zones, if any, were determined, using tetracycline as the positive control. The minimum inhibitory concentration (MIC) values for compounds that showed significant inhibition zones were further determined in the 96-well plate with Müller-Hinton (MH) broth (supplemented with 20 mg $Ca^{2+}$ and 10 mg $Mg^{2+}$ per liter).[37, 38] The tested strains were grown in MH broth to early stationary phase, diluted by MH broth to an $OD_{625}$ = 0.005, then pipeted into the 96-well plate with 100 μL of broth in each well. The tested compounds with different concentrations were added into different wells, using the wells containing no compounds or containing tetracycline as negative and positive controls, respectively. The final DMSO concentration in each well was 1%, which did not affect the growth of any of the tested strains. The MIC values were determined after incubation at 37 °C for 18 h, using a plate reader at $OD_{625}$.

## Supplementary Material

Refer to Web version on PubMed Central for supplementary material.

## Acknowledgments

This work is supported in part by the Natural Products Library Initiative at The Scripps Research Institute, NIH grant GM086184 (to B.S.), the Chinese Ministry of Education 111 Project B08034 (to Y.D.), and National High Technology Joint Research Program of China grant 2011ZX09401-001 (to Y.D.).

## REFERENCES

1. Kharel MK, Pahari P, Shepherd MD, Tibrewal N, Nybo SE, Shaaban KA, Rohr J. Nat. Prod. Rep. 2012; 29:264–325. [PubMed: 22186970]
2. Rohr J, Thiericke R. Nat. Prod. Rep. 1992; 9:103–137. [PubMed: 1620493]

3. Kalinovskaya NI, Kalinovsky AI, Romanenko LA, Pushilin MA, Dmitrenok PS, Kuznetsova TA. Nat. Prod. Commun. 2008; 3:1611–1616.
4. Fotso S, Mahmud T, Zabriskie TM, Santosa DA, Sulastri Proteau PJ. J. Nat. Prod. 2008; 71:61–65. [PubMed: 18081255]
5. Izawa M, Kimata S, Maeda A, Kawasaki T, Hayakawa Y. J. Antibiot. 2014; 67:159–162. [PubMed: 24129687]
6. Rix U, Zheng J, Remsing RLL, Greenwell L, Yang K, Rohr J. J. Am. Chem. Soc. 2004; 126:4496–4497. [PubMed: 15070349]
7. Drautz H, Zahner H, Rohr J, Zeeck A. J. Antibiot. 1986; 39:1657–1669. [PubMed: 3818439]
8. Huang H, Yang T, Ren X, Liu J, Song Y, Sun A, Ma J, Wang B, Zhang Y, Huang C, Zhang C, Ju J. J. Nat. Prod. 2012; 75:202–208. [PubMed: 22304344]
9. Balitz DM, O' Herron FA, Bush J, Vyas DM, Nettleton DE, Grulich RE, Bradner WT, Doyle TW, Arnold E, Clardy J. J. Antibiot. 1981; 34:1544–1555. [PubMed: 7344705]
10. Gerlitz M, Udvarnoki G, Rohr J. Angew. Chem. Int. Ed. Engl. 1995; 34:1617–1621.
11. Henkel T, Rohr J, Beale JM, Schwenen L. J. Antibiot. 1990; 43:492–503. [PubMed: 2358402]
12. Uchida T, Imoto M, Watanabe Y, Miura K, Dobashi T, Matsuda N, Sawa T, Naganawa H, Hamada M, Takeuchi T. J. Antibiot. 1985; 38:1171–1181. [PubMed: 3840796]
13. Yu Z, Vodanovic-Jankovic S, Ledeboer N, Huang SX, Rajski SR, Kron M, Shen B. Org. Lett. 2011; 13:2034–2037. [PubMed: 21405052]
14. Zhao LX, Huang SX, Tang SK, Jiang CL, Duan Y, Beutler JA, Henrich CJ, McMahon JB, Schmid T, Blees JS, Colburn NH, Rajski SR, Shen B. J. Nat. Prod. 2011; 74:1990–1995. [PubMed: 21870828]
15. Yu Z, Rateb ME, Smanski MJ, Peterson RM, Shen B. J. Antibiot. 2013; 66:291–294. [PubMed: 23361357]
16. Rateb ME, Yu Z, Yan Y, Yang D, Huang T, Vodanovic-Jankovic S, Kron MA, Shen B. J. Antibiot. 2014; 67:127–132. [PubMed: 23715040]
17. (a) Xie P, Ma M, Rateb ME, Shaaban KA, Yu Z, Huang SX, Zhao LX, Zhu X, Yan Y, Peterson RM, Lohman JR, Yang D, Yin M, Rudolf JD, Jiang Y, Duan Y, Shen B. J. Nat. Prod. 2014; 77:337–387.(b) Hindra, Huang T, Yang D, Rudolf JD, Xie P, Xie G, Teng Q, Lohman JR, Zhu X, Huang Y, Zhao L-X, Jiang Y, Duan Y, Shen B. J. Nat. Prod. 2014; 77:2296–2303. 190. [PubMed: 25238028]
18. (a) Maruna M, Sturdikova M, Liptaj T, Godany A, Muckova M, Certik M, Pronayova N, Proksa B. J. Basic Microbiol. 2010; 50:135–142. [PubMed: 20082376] (b) Gilpin ML, Balchin J, Box SJ, Tyler JW. J. Antibiot. 2006; 42:627–628. [PubMed: 2722675] (c) Kesenheimer C, Groth U. Org. Lett. 2006; 8:2507–2510. [PubMed: 16737300]
19. Nakajima S, Kojiri K, Suda H, Okanishi M. J. Antibiot. 1991; 44:1061–1064. [PubMed: 1955387]
20. Fotso S, Mahmud T, Zabriskie M, Santosa DA, Proteau PJ. J. Antibiot. 2008; 61:449–456. [PubMed: 18776657]
21. Carr G, Derbyshire ER, Caldera E, Currie CR, Clardy J. J. Nat. Prod. 2012; 75:1806–1809. [PubMed: 23025282]
22. Guo ZK, Liu SB, Jiao RH, Wang T, Tan RX, Ge HM. Bioorg. Med. Chem. Lett. 2012; 22:7490–7493. [PubMed: 23131338]
23. Chen C, Song F, Guo H, Abdel-Mageed WM, Bai H, Dai H, Liu X, Wang J, Zhang L. J. Antibiot. 2012; 65:433–435. [PubMed: 22569162]
24. Xie ZP, Zhang HY, Li FC, Liu B, Yang SX, Wang HP, Pu Y, Chen Y, Qin S. Chin. Chem. Lett. 2012; 23:941–944.
25. (a) Shaaban KA, Stamatkin C, Damodaran C, Rohr J. J. Antibiot. 2007; 2007; 64:141–150. [PubMed: 20978514] (b) Kaliappan K, Ravikumar V. J. Org. Chem. 72:6116–6126. [PubMed: 17625884]
26. Kalyon B, Tan GYA, Pinto JM, Foo CY, Wiese J, Imhoff JF, Sussmuth RD, Sabaratnam V, Fiedler HP. J. Antibiot. 2013; 66:609–616. [PubMed: 23820614]
27. Guo ZK, Wang T, Guo Y, Song YC, Tan RX, Ge HM. Planta Med. 2011; 77:2057–2060. [PubMed: 21830188]

28. Igarashi M, Watanabe T, Hashida T, Umekita M, Hatano M, Yanagida Y, Kino H, Kimura T, Kinoshita N, Inoue K, Sawa R, Nishimura Y, Utsumi R, Nomoto A. J. Antibiot. 2013; 66:459–464. [PubMed: 23632918]
29. Jakeman DL, Bandi S, Graham CL, Reid TR, Wentzell JR, Douglas SE. Antimicrob. Agents Chemother. 2009; 53:1245–1247. [PubMed: 19075054]
30. Theriault RJ, Rasmussen RR, Kohl WL, Prokop JF, Hutch TB, Barlow GJ. J. Antibiot. 1986; 39:1509–1514. [PubMed: 3793619]
31. Okazaki T, Kitahara T, Okami Y. J. Antibiot. 1975; 28:176–184. [PubMed: 1126873]
32. Carr G, Derbyshire ER, Caldera E, Currie CR, Clardy J. J. Nat. Prod. 2012; 75:1806–1809. [PubMed: 23025282]
33. Gilpin ML, Balchin J, Box SJ, Tyler JW. J. Antibiot. 2012; 42:627–628. [PubMed: 2722675]
34. Sakai K, Koyama N, Fukuda T, Mori Y, Onaka H, Tomoda H. Biol. Pharm. Bull. 2012; 35:48–53. [PubMed: 22223336]
35. Zhang DF, Pan HQ, He J, Zhang XM, Zhang YG, Klenk HP, Hu JC, Li WJ. Int. J. Syst. Evol. Microbiol. 2013; 63:4447–4455. [PubMed: 23847283]
36. Thornsberry C, Barry AL, Jones RN, Baker CN, Badal RE. J. Clin. Microbiol. 1982; 15:769–776. [PubMed: 6212595]
37. Rateb ME, Houssen WE, Harrison WT, Deng H, Okoro CK, Asenjo JA, Andrews BA, Bull AT, Goodfellow M, Ebel R, Jaspars M. J. Nat. Prod. 2011; 74:1965–1971. [PubMed: 21879726]
38. Wiegand I, Hilpert K, Hancock REW. Nat. Protoc. 2008; 3:163–175. [PubMed: 18274517]

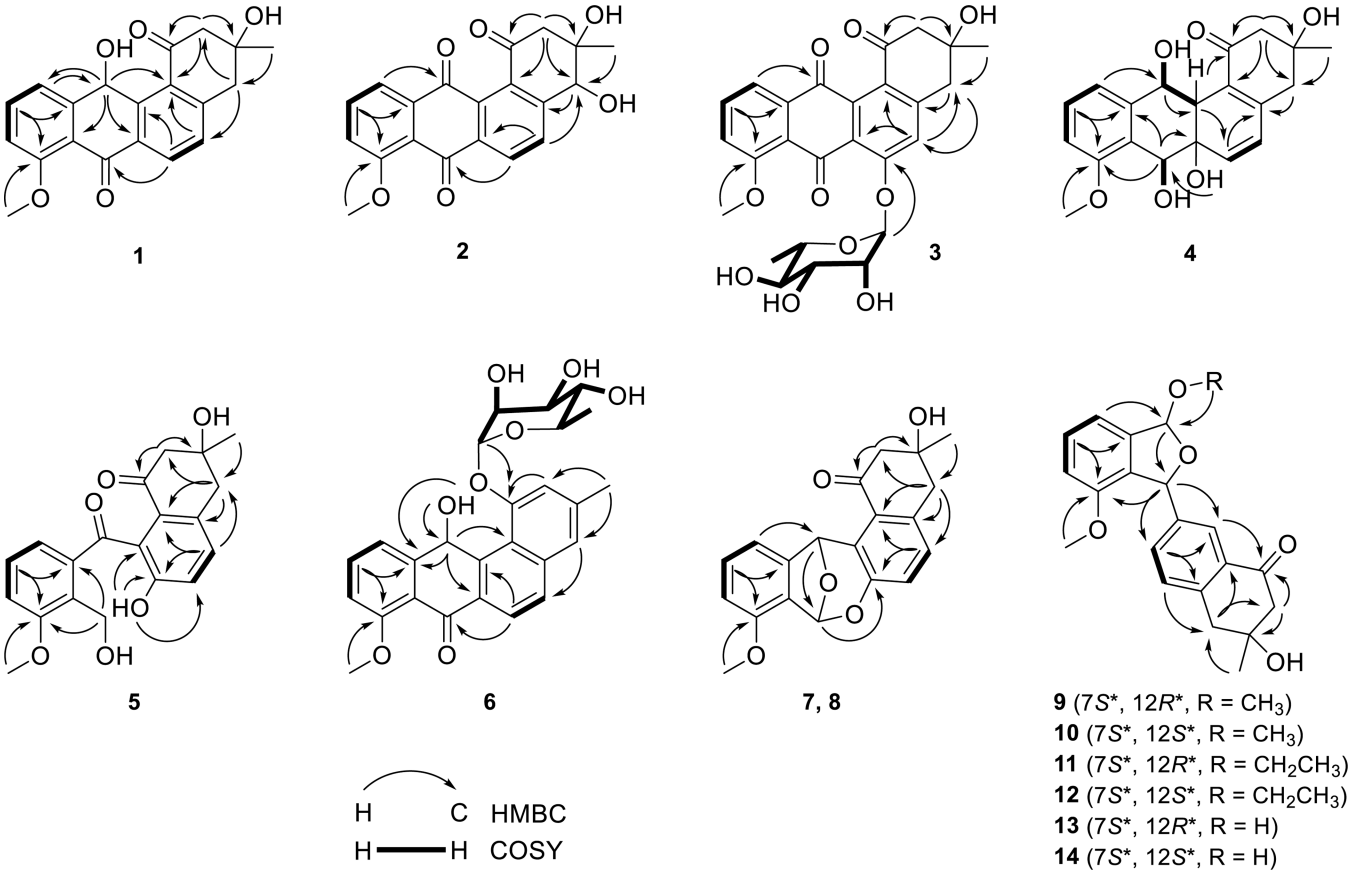


**Figure 1.**
Key COSY and HMBC correlations supporting structural assignments of **1–14**.

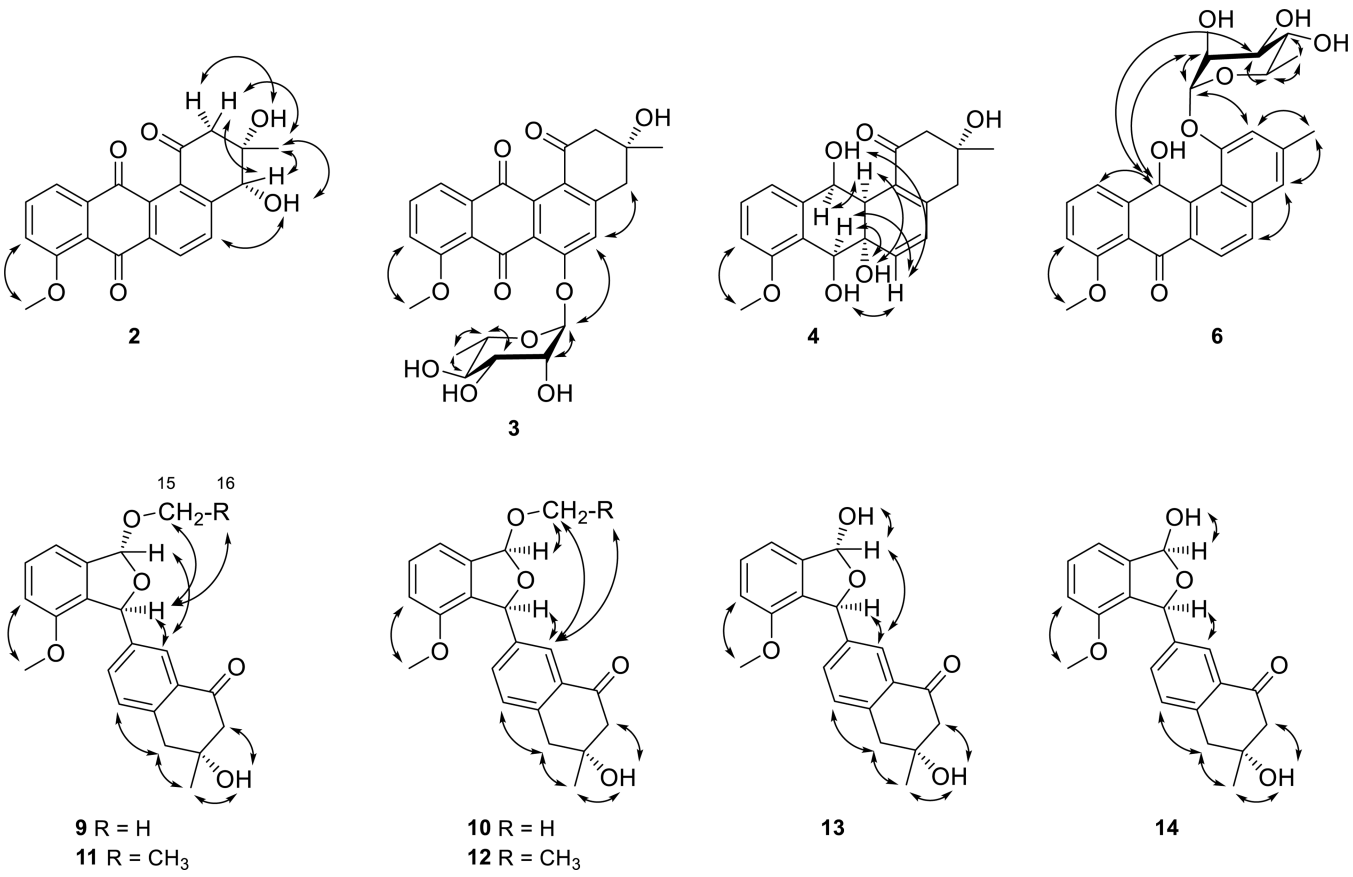


**Figure 2.**
Key NOESY correlations supporting the relative configurations of **2–4, 6**, and **9–14**.

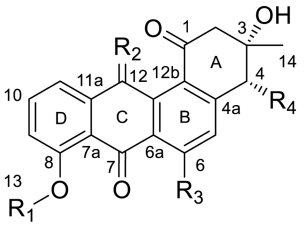

**1** ($R_1$ = $CH_3$, $R_2$ = OH, H, $R_3$ = $R_4$ = H)
**2** ($R_1$ = $CH_3$, $R_2$ = O, $R_3$ = H, $R_4$ = OH)
**3** ($R_1$ = $CH_3$, $R_2$ = O, $R_3$ = ORha, $R_4$ = H)
**15** ($R_1$ = H, $R_2$ = O, $R_3$ = $R_4$ = H)
**16** ($R_1$ = $CH_3$, $R_2$ = O, $R_3$ = $R_4$ = H)

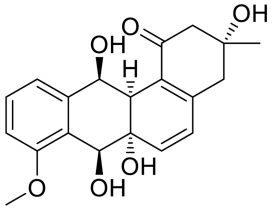

**4**

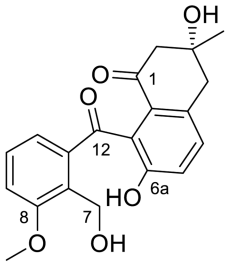

**5**

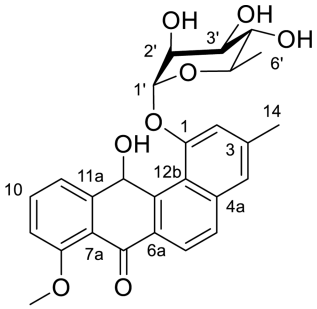

**6**

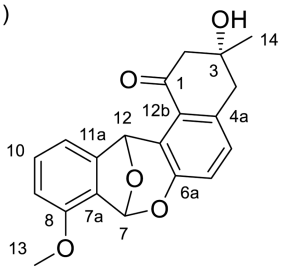

**7, 8** (7*R*, 12*R* or 7*S*, 12*S*)

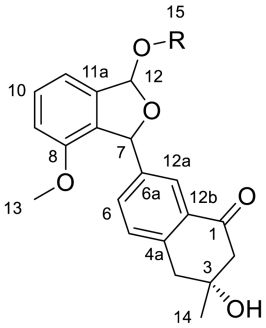

**9** (7*S**, 12*R**, R = $CH_3$)
**10** (7*S**, 12*S**, R = $CH_3$)
**11** (7*S**, 12*R**, R = $CH_2CH_3$)
**12** (7*S**, 12*S**, R = $CH_2CH_3$)
**13** (7*S**, 12*R**, R = H)
**14** (7*S**, 12*S**, R = H)

**Chart 1.**

**Table 1**

$^1$H (700 MHz) NMR Data ($\delta_H$, *J* in Hz) for **1–2**, **4–5**, and **7–8** in DMSO-$d_6$[a]

| position | 1 | 2 | 4 | 5 | 7 | 8 |
|---|---|---|---|---|---|---|
| 2 | 2.93, d (14.9) | 3.05, d (14.9) | 2.55, d (15.6) | 2.64, br s | 2.94, d (15.1) | 2.67, d (16.6) |
| | 2.73, dd (14.9, 2.2) | 2.77, d (14.9) | 2.43, d (15.6) | 2.46, dd (16.2, 1.8) | 2.59, dd (15.1, 2.2) | 2.72, dd (16.6, 1.8) |
| 4 | 3.22, d (16.9) | 4.72, s | 2.65, d (16.7) | 3.04, d (16.3) | 3.05, d (16.2) | 2.95, d (16.1) |
| | 3.11, dd (16.9, 1.8) | | 2.58, d (16.7) | 2.91, dd (16.3, 1.5) | 2.83, dd (16.5, 1.9) | 2.87, dd (16.2, 1.3) |
| 5 | 7.49, d (8.0) | 8.05, d (8.1) | 6.03, d (10.1) | 7.27, d (8.3) | 7.11, d (8.3) | 7.14, d (8.3) |
| 6 | 8.10, d (8.1) | 8.23, d (8.2) | 6.31, d (10.1) | 7.17, d (8.3) | 6.91, d (8.3) | 6.92, d (8.3) |
| 7 | | | 4.83, br d (9.7) | 4.85, s | 6.84, s | 6.85, s |
| 9 | 7.15, d (8.1) | 7.57, d (8.0) | 7.00, d (7.9) | 7.19, dd (8.2, 1.8) | 6.97, d (8.2) | 6.96, d (8.3) |
| 10 | 7.63, dd (8.2, 7.6) | 7.85, t (8.0) | 7.28, t (8.1) | 7.24, t (7.8) | 7.29, dd (8.2, 7.4) | 7.27, dd (8.2, 7.4) |
| 11 | 7.22, d (7.4) | 7.57, d (8.0) | 6.90, d (7.9) | 6.83, br s | 7.14, d (7.4) | 7.05, d (7.3) |
| 12 | 6.39, s | | 4.86, br s | | 6.64, s | 6.80, s |
| 12a | | | 2.67, br s | | | |
| 13 | 3.88, s | 3.96, s | 3.81, s | 3.85, s | 3.86, s | 3.86, s |
| 14 | 1.32, s | 1.34, s | 1.20, s | 1.25, s | 1.30, s | 1.23, s |
| 3-OH | | 4.82, br s | 4.82, s | 4.78, br s | 4.74, s | 4.85, s |
| 4-OH | | 5.93, br s | | | | |
| 6a-OH | | | 5.15, s | 9.89, s | | |
| 7-OH | | | 5.24, br d (9.3) | 4.78, br s | | |
| 12-OH | | | 5.48, br s | | | |

[a]Assignments are based on COSY, HMBC, HSQC, and NOESY experiments.

**Table 2**

$^1$H (700 MHz) NMR Data ($\delta_H$, *J* in Hz) for **3** and **6** in DMSO-$d_6$[a]

| position | 3 | 6 | position | 3 | 6 |
|---|---|---|---|---|---|
| 2 | 2.91, d (14.4), 2.69, dd (14.4, 1.6) | 7.31, d (1.3) | 1' | 5.66, br s [d (1.7)][b] | 5.60, d (1.7) [d (1.8)][b] |
| 4 | 3.14, d (16.7), 3.01, dd (16.7, 1.2) | 7.43, br s | 2' | 3.98, dd (3.2, 1.8) [dd (3.4, 1.8)][b] | 4.41, br s [dd (3.4, 1.9)][b] |
| 5 | 7.38, s | 7.88, d (8.7) | 3' | 3.90, dd (9.5, 3.2) [dd (9.5, 3.4)][b] | 3.97, br s [dd (9.2, 3.5)][b] |
| 6 | | 8.02, d (8.6) | 4' | 3.36, t (9.4) [t (9.5)][b] | 3.42, m [t (9.2)][b] |
| 9 | 7.51, d (8.5) | 7.18, d (8.1) | 5' | 3.55, m | 3.62, m |
| 10 | 7.76, t (8.0) | 7.65, br t (8.2) | 6' | 1.13, d (6.2) | 1.23, d (6.2) |
| 11 | 7.44, d (7.5) | 7.29, d (7.4) | 3-OH | 5.00, br s | |
| 12 | | 6.86, d (6.5) | 12-OH | | 5.56, d (6.6) |
| 13 | 3.93, s | 3.90, s | 2'-OH | 5.00, br s | 5.15, d (4.1) |
| 14 | 1.31, s | 2.46, s | 3'-OH | 5.00, br s | 4.96, br d (5.4) |
| | | | 4'-OH | 5.00, br s | 4.97, br d (6.0) |

[a] Assignments are based on COSY, HMBC, HSQC, and NOESY experiments.

[b] Coupling constants in square brackets are calculated after $D_2O$ was added into DMSO-*d6*.

**Table 3**

$^{1}$H (700 MHz) NMR Data ($\delta_H$, *J* in Hz) for **9–14** in DMSO-$d_6$[a]

| position | 9 | 10 | 11 | 12 | 13 | 14 |
|---|---|---|---|---|---|---|
| 2 | 2.73, d (16.1) | 2.72, d (16.0) | 2.73, d (16.1) | 2.71, d (16.0) | 2.72, d (16.1) | 2.73, d (16.1) |
| | 2.59, dd (16.1, 2.1) | 2.59, dd (16.0, 1.8) | 2.59, dd (16.1, 2.1) | 2.59, dd (16.0, 2.0) | 2.59, dd (16.1, 2.1) | 2.60, dd (16.0, 2.0) |
| 4 | 3.11, d (16.5) | 3.10, d (16.5) | 3.10, d (16.5) | 3.09, d (16.5) | 3.09, d (16.5) | 3.10, d (16.6) |
| | 2.95, dd (16.6, 1.8) | 2.94, br d (16.5) | 2.94, dd (16.7, 1.8) | 2.94, dd (16.6, 1.8) | 2.93, dd (16.5, 2.1) | 2.94, dd (16.3, 2.1) |
| 5 | 7.28, d (7.9) | 7.27, d (7.8) | 7.28, d (7.9) | 7.27, d (7.8) | 7.25, d (8.3) | 7.27, d (8.7) |
| 6 | 7.45, dd (7.8, 2.0) | 7.51, dd (7.8, 1.7) | 7.45, dd (7.9, 2.0) | 7.57, dd (7.9, 2.0) | 7.44, dd (7.9, 2.0) | 7.62, dd (7.9, 1.9) |
| 7 | 6.33, d (2.2) | 6.18, s | 6.31, d (2.3) | 6.17, s | 6.26, d (2.2) | 6.08, s |
| 9 | 6.98, d (8.1) | 6.98, d (8.1) | 6.97, d (8.1) | 6.96, d (8.1) | 6.92, d (8.1) | 6.94, d (8.1) |
| 10 | 7.41, t (8.1) | 7.39, t (7.7) | 7.40, t (8.0) | 7.37, br t (8.0) | 7.38, t (8.0) | 7.36, t (8.0) |
| 11 | 7.06, d (7.6) | 7.05, d (7.5) | 7.05, d (7.6) | 7.03, d (7.5) | 7.03, d (7.5) | 7.01, d (7.5) |
| 12 | 6.43, d (2.3) | 6.13, s | 6.48, d (2.3) | 6.22, s | 6.58, br d (5.1) | 6.43, d (5.0) |
| 12a | 7.69, d (1.9) | 7.89, d (1.5) | 7.67, d (2.0) | 7.96, d (1.9) | 7.68, d (1.9) | 7.96, d (1.8) |
| 13 | 3.63, s | 3.66, s | 3.62, s | 3.66, s | 3.63, s | 3.64, s |
| 14 | 1.29, s | 1.29, s | 1.29, s | 1.29, s | 1.28, s | 1.29, s |
| 15 | 3.30, s | 3.43, s | 3.61, q (7.5) | 3.82, dq (9.5, 7.1) | | |
| | | | | 3.69, dq (9.6, 7.0) | | |
| 16 | | | 1.16, t (7.1) | 1.23, t (7.1) | | |
| 3-OH | 4.79, s | 4.79, s | 4.78, s | 4.78, s | 4.79, s | 4.79, s |
| 12-OH | | | | | 6.88, d (7.4) | 7.23, d (5.5) |

[a]Assignments are based on COSY, HMBC, HSQC, and NOESY experiments.

**Table 4**

$^{13}$C (175 MHz) NMR Data ($\delta_C$, type) for **1–8** in DMSO-$d_6$[a]

| position | 1 | 2 | 3 | 4 | 5 | 6 | 7 | 8 |
|---|---|---|---|---|---|---|---|---|
| 1 | 200.4, C | 196.2, C | 196.2, C | 197.7, C | 198.1, C | 155.8, C | 200.2, C | 200.0, C |
| 2 | 54.4, $CH_2$ | 52.3, $CH_2$ | 53.4, $CH_2$ | 52.4, $CH_2$ | 52.1, $CH_2$ | 113.6, CH | 53.5, $CH_2$ | 53.3, $CH_2$ |
| 3 | 70.8, C | 74.9, C | 71.6, C | 69.7, C | 70.9, C | 139.0, C | 71.6, C | 69.9, C |
| 4 | 44.7, $CH_2$ | 73.8, CH | 44.1, $CH_2$ | 44.3, $CH_2$ | 42.5, $CH_2$ | 122.0, CH | 43.0, $CH_2$ | 43.2, $CH_2$ |
| 4a | 148.6, C | 151.6, C | 149.5, C | 146.5, C | 134.0, C | 137.8, C | 135.1, C | 135.2, C |
| 5 | 130.5, CH | 132.4, CH | 120.3, CH | 124.7, CH | 131.6, CH | 128.8, CH | 130.3, CH | 130.5, CH |
| 6 | 131.1, CH | 129.5, CH | 157.2, C | 138.7, CH | 122.1, CH | 123.6, CH | 122.3, CH | 122.6, CH |
| 6a | 133.7, C | 135.0, C | 124.0, C | 71.4, C | 153.0, C | 131.9, C | 148.2, C | 148.3, C |
| 7 | 183.2, C | 180.7, C | 180.1, C | 67.7, CH | 54.9, $CH_2$ | 183.7, C | 99.0, CH | 99.1, CH |
| 7a | 120.2, C | 120.4, C | 123.1, C | 127.4, C | 129.9, C | 120.3, C | 123.3, C | 123.2, C |
| 8 | 159.7, C | 135.0, C | 158.7, C | 156.9, C | 158.2, C | 159.5, C | 154.0, C | 154.1, C |
| 9 | 112.5, CH | 118.8, CH | 118.5, CH | 111.0, CH | 115.4, CH | 112.4, CH | 112.0, CH | 112.0, CH |
| 10 | 135.1, CH | 136.3, CH | 135.2, CH | 128.5, CH | 128.6, CH | 134.8, CH | 131.8, CH | 131.9, CH |
| 11 | 122.5, CH | 118.9, CH | 117.7, CH | 119.6, CH | 122.8, CH | 122.6, CH | 112.3, CH | 111.9, CH |
| 11a | 146.4, C | 137.7, C | 136.9, C | 142.6, C | 139.3, C | 146.9, C | 148.7, C | 148.7, C |
| 12 | 64.3, CH | 184.6, C | 186.2, C | 70.1, CH | 199.8, C | 65.2, CH | 77.7, CH | 77.6, CH |
| 12a | 142.0, C | 134.5, C | 138.9, C | 46.6, CH | 128.1, C | 139.6, C | 126.3, C | 126.5, C |
| 12b | 130.1, C | 134.1, C | 127.9, C | 125.8, C | 130.6, C | 120.7, C | 127.6, C | 127.1, C |
| 13 | 56.3, $CH_3$ | 56.9, $CH_3$ | 56.9, $CH_3$ | 55.6, $CH_3$ | 56.5, $CH_3$ | 56.3, $CH_3$ | 56.0, $CH_3$ | 56.0, $CH_3$ |
| 14 | 29.6, $CH_3$ | 26.8, $CH_3$ | 30.6, $CH_3$ | 28.4, $CH_3$ | 29.6, $CH_3$ | 22.0, $CH_3$ | 30.1, $CH_3$ | 29.1, $CH_3$ |
| 1' | | | 99.4, CH | | | 100.9, CH | | |
| 2' | | | 70.4, CH | | | 70.4, CH | | |
| 3' | | | 70.4, CH | | | 72.0, CH | | |
| 4' | | | 72.1, CH | | | 72.5, CH | | |
| 5' | | | 70.7, CH | | | 70.4, CH | | |
| 6' | | | 18.4, $CH_3$ | | | 18.5, $CH_3$ | | |

[a]Assignments are based on COSY, HMBC, HSQC, and NOESY experiments.

**Table 5**

$^{13}$C (175 MHz) NMR Data ($\delta_C$, type) for **9–14** in DMSO-$d_6$[a]

| position | 9 | 10 | 11 | 12 | 13 | 14 |
|---|---|---|---|---|---|---|
| 1 | 197.8, C | 197.7, C | 197.7, C | 197.7, C | 197.8, C | 197.8, C |
| 2 | 52.3, $CH_2$ | 52.4, $CH_2$ | 52.3, $CH_2$ | 52.4, $CH_2$ | 52.3, $CH_2$ | 52.4, $CH_2$ |
| 3 | 70.9, C | 70.9, C | 70.9, C | 70.9, C | 70.9, C | 71.0, C |
| 4 | 42.9, $CH_2$ | 42.9, $CH_2$ | 42.9, $CH_2$ | 42.9, $CH_2$ | 42.8, $CH_2$ | 42.9, $CH_2$ |
| 4a | 142.2, C | 142.0, C | 142.2, C | 141.9, C | 141.9, C | 141.8, C |
| 5 | 129.9, CH | 129.8, CH | 129.9, CH | 129.5, CH | 129.8, CH | 129.8, CH |
| 6 | 133.1, CH | 133.1, CH | 133.1, CH | 133.1, CH | 133.0, CH | 133.4, CH |
| 6a | 139.4, C | 139.6, C | 139.4, C | 139.9, C | 140.0, C | 140.3, C |
| 7 | 83.8, CH | 83.8, CH | 83.6, CH | 83.9, CH | 82.7, CH | 83.2, CH |
| 7a | 130.1, C | 129.9, C | 130.0, C | 130.1, C | 129.7, C | 129.5, C |
| 8 | 154.4, C | 154.4, C | 154.4, C | 154.3, C | 154.3, C | 154.3, C |
| 9 | 112.2, CH | 112.0, CH | 112.1, CH | 111.8, CH | 111.6, CH | 111.4, CH |
| 10 | 131.0, CH | 130.8, CH | 130.9, CH | 130.7, CH | 130.7, CH | 130.6, CH |
| 11 | 115.5, CH | 115.5, CH | 115.5, CH | 115.5, CH | 115.3, CH | 115.4, CH |
| 11a | 139.7, C | 139.7, C | 140.2, C | 139.8, C | 142.7, C | 142.0, C |
| 12 | 107.2, CH | 107.6, CH | 106.3, CH | 106.4, CH | 101.3, CH | 101.0, CH |
| 12a | 124.8, CH | 125.3, CH | 124.8, CH | 125.5, CH | 124.6, CH | 125.5, CH |
| 12b | 132.0, C | 131.9, C | 132.0, C | 132.0, C | 131.9, C | 131.7, C |
| 13 | 55.9, $CH_3$ | 55.9, $CH_3$ | 55.9, $CH_3$ | 55.9, $CH_3$ | 55.8, $CH_3$ | 55.9, $CH_3$ |
| 14 | 29.9, $CH_3$ | 29.9, $CH_3$ | 29.9, $CH_3$ | 29.9, $CH_3$ | 29.8, $CH_3$ | 29.9, $CH_3$ |
| 15 | 53.8, $CH_3$ | 55.5, $CH_3$ | 62.4, $CH_2$ | 63.7, $CH_2$ | | |
| 16 | | | 15.8, $CH_3$ | 15.7, $CH_3$ | | |

[a]Assignments are based on COSY, HMBC, HSQC, and NOESY experiments.

**Table 6**

Cytotoxicity and Antibacterial Assays for **1, 5, 15** and **16**

| | cytotoxicity ($IC_{50}$, μM) | | | | | antibacterial activity (MIC, μg/mL) | | |
|---|---|---|---|---|---|---|---|---|
| | **SF295** | **H226** | **SF539** | **M14** | **MDA-MB-468** | ***S. aureus*** | ***B. subtilis*** | ***M. smegmatis*** |
| **1** | 3.1±0.1 | 7.2±0.4 | 12±2 | 31±6 | 52±1 | >100 | >100 | >100 |
| **5** | >100 | >100 | >100 | >100 | >100 | >100 | 85 | 93 |
| **15** | 12±1 | 7.2±0.5 | 3.2±0.2 | 2.4±0.1 | 16±1 | 11 | 8.1 | 9.7 |
| **16** | 17±1 | 4.6±0.3 | 10±1 | 9.7±0.6 | 27±1 | >100 | 25 | >100 |
| mitomycin C | 0.54±0.01 | 0.58±0.02 | $(3.8\pm0.3)\times10^{-2}$ | 0.47±0.01 | 0.50±0.02 | N | N | N |
| tetracycline | N | N | N | N | N | 6.7 | 13 | 11 |

“N” indicates compounds not tested.